FEBS Letters 392 (1996) 110–113 FEBS 17403

Molecular imaging of *Escherichia coli* F_0F_1-ATPase in reconstituted membranes using atomic force microscopy

Kunio Takeyasu[a,b,*], Hiroshi Omote[c], Saju Nettikadan[a], Fuyuki Tokumasu[a,b], Atsuko Iwamoto-Kihara[c], Masamitsu Futai[c]

[a] *Department of Medical Biochemistry, and Neurobiotechnology Center, The Ohio State University, Columbus, OH 43210, USA*
[b] *Department of Natural Environment Sciences, Faculty of Integrated Human Studies, Kyoto University, Yoshida Nihonmatsu, Kyoto 606-01, Japan*
[c] *Division of Biological Science, The Institute of Scientific and Industrial Research, Osaka University, Ibaraki, Osaka 567, Japan*

Received 16 June 1996

Abstract The structure of *Escherichia coli* F_0F_1-ATPase (ATP synthase), and its F_0 sector reconstituted in lipid membranes was analyzed using atomic force microscopy (AFM) by tapping-mode operation. The majority of F_0F_1-ATPases were visualized as spheres with a calculated diameter of ~90 Å, and a height of ~100 Å from the membrane surface. F_0 sectors were visualized as two different ring-like structures (one with a central mass and the other with a central hollow of ≥18 Å depth) with a calculated outer diameter of ~130 Å. The two different images possibly represent the opposite orientations of the complex in the membranes. The ring-like projections of both images suggest inherently asymmetric assemblies of the subunits in the F_0 sector. Considering the stoichiometry of F_0 subunits, the area of the image observed is large enough to accommodate all three F_0 subunits in an asymmetric manner.

Key words: AFM; F_0F_1-ATPase; ATP synthase; H^+-channel; Subunit assembly

1. Introduction

The F_0F_1-ATPase (ATP synthase) of bacteria, mitochondria and chloroplasts catalyzes ATP synthesis, and is a large complex formed from the catalytic F_1 sector and the transmembrane proton-channel, F_0 sector [1–3]. Sufficient structural information on the F_1 sector has been obtained by electron microscopy [4–6] and X-ray crystallography [7,8]. The higher-ordered structure of the catalytic subunit complex is consistent with the binding-change mechanism of ATP synthesis [9].

The bacterial F_0 sector is composed of *a*, *b* and *c* subunits with a stoichiometry of 1:2:10–12, and all three subunits are necessary to reconstitute a functional sector [2,10]. Each subunit of F_0 traverses the membrane; subunit *a* is very hydrophobic and crosses the membrane several times (perhaps 6 times), whereas subunit *b* may cross the membrane with a single transmembrane helix, leaving a polar domain exposed to the cytoplasm. This polar domain along with parts of F_1 subunits constitutes the stalk region connecting F_1 and F_0. Subunit *c* has a hairpin structure with two transmembrane helical domains with a polar cytoplasmic loop in between. NMR spectroscopy [11,12] supports a transmembrane hairpin model for subunit *c*. Asp-61 of the *c* subunit is known to be critical for the formation of a proton pathway together with the specific *a* subunit residues [1,2].

In this study, *Escherichia coli* F_0 and F_0F_1 complexes were imaged using atomic force microscopy (AFM). The AFM images were critically evaluated and a model of F_0 is proposed.

2. Materials and methods

2.1. Reconstitution of purified F_0 and F_0F_1-ATPase in lipid membranes

F_0F_1-ATPase was purified from membranes of *E. coli* strain DK8 carrying pBWU13: >95% pure, as judged on polyacrylamide gel electrophoresis in the presence of sodium dodecyl sulfate [13]. The F_0 sector was purified using urea as described previously [14]. The purified F_0F_1-ATPase and its F_0 sector were reconstituted with phospholipids (protein/lipid ratio, 1:1) and the reconstituted membranes exhibited ATPase activity of 30.8 units (μmol/min per mg), and showed significant proton transport activity, respectively [13].

2.2. Preparation of specimens for atomic force microscopy (AFM)

Electron microscopy of a negatively stained specimen revealed the high quality of the membrane preparations. The membrane preparations (2 mg protein/ml) were spread on a freshly cleaved mica surface for 5 min, rinsed with water, dried for a few hours to remove excess water, and then imaged by AFM. In some experiments, the membranes were treated with 1% aqueous uranyl acetate as described previously [15]. This procedure gave the samples mechanical strength.

2.3. AFM

Samples were imaged using AFM by the tapping-mode. The free vibrating amplitude was set at about 3 V and the set point was defined as 2.25 V (about 3/4 of the free vibrating amplitude). Data were collected immediately upon finding an area of interest. The images were stored in a 256×256 pixel format. Quantitative data were obtained by analyzing orthogonal sections of the images at 200 nm. No filtering or enhancement was performed to augment the obtained images. Both data acquisition and analysis were performed with Nanoscope III software (Digital Instruments).

3. Results and discussion

3.1. Imaging F_0 and F_0F_1-ATPase in reconstituted membranes

Examination of reconstituted lipid membranes by electron microscopy (EM) revealed that the F_0F_1-ATPase with a F_1 sector of about 90 Å diameter was distributed randomly within a given membrane vesicle (data not shown). The surface topology of the membranes studied by AFM revealed that F_0F_1-ATPases were frequently observed as pairs of spheres (Fig. 1A,C). However, these pairs of F_0F_1 molecules were reasonably well separated from each other, and the height of individual molecules (dimers) was measured to be (97 ± 15 Å; mean ± S.D. for 50 individual molecules). In contrast to the images of F_1 sectors, AFM images of F_0 sectors did not show any large particles like F_1. The height of the F_0 sector out of the membrane was measured to be very small (< 10 Å) (Table 1). Instead, two ring-like structures were consistently observed; one with a central hollow of ≥ 18 Å depth, and a similar one with a central mass (Fig. 1B,D). A

*Corresponding author. Fax: (1) (614) 292-8542.

PII S0014-5793(96)00796-X

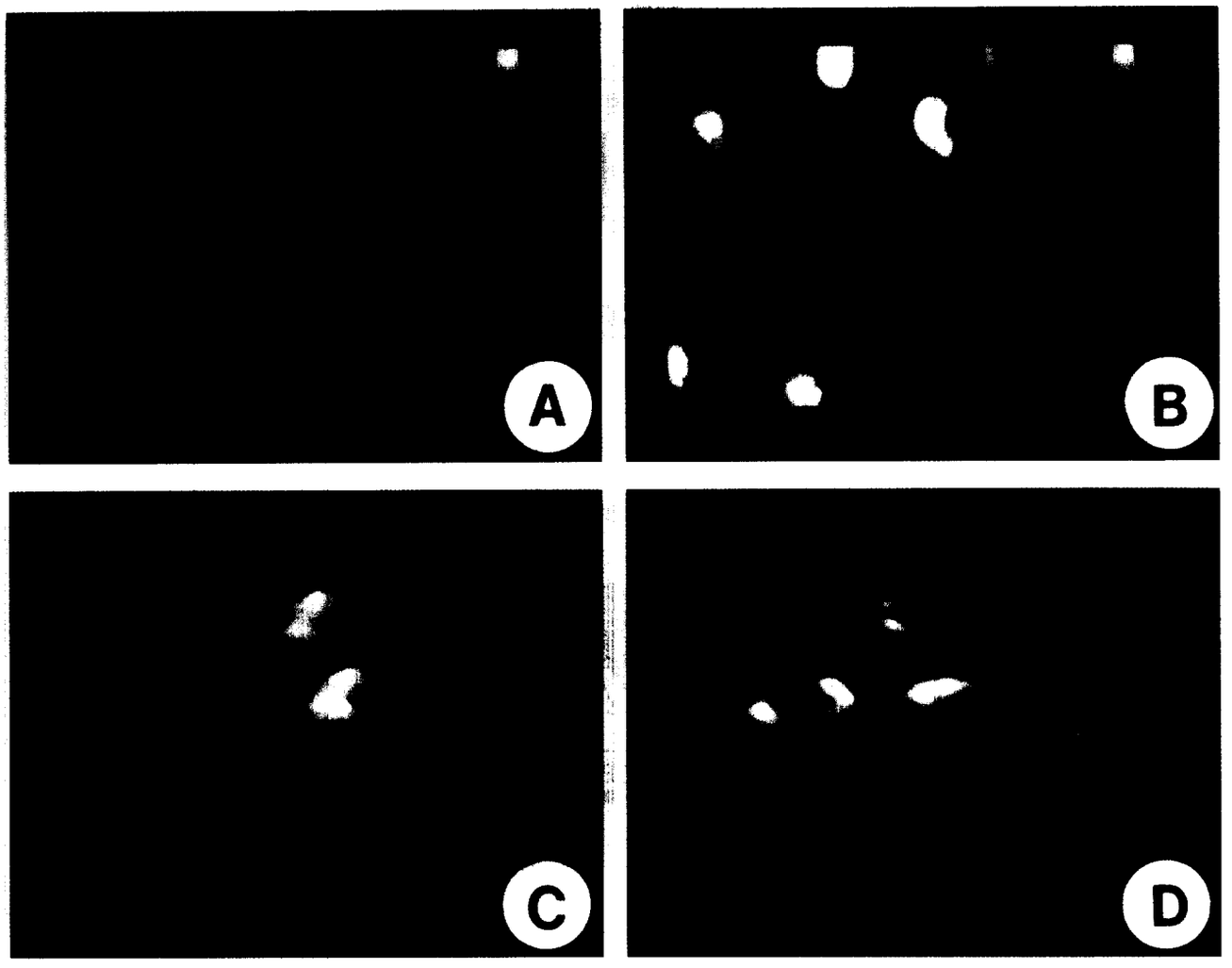

Fig. 1. Molecular imaging of F_0F_1 (A,C) and F_0 sectors (B,D) by AFM. The reconstituted membranes were adsorbed onto a mica surface, and imaged after staining with 1% uranyl acetate. The images obtained were direct 500 nm scans of the samples. (A) Several dozens of F_0F_1-ATPase molecules with F_1 sectors facing the scanning tip. (B) Several dozens of F_0 sectors exhibiting ring-like structures: one with a hollow and the other with a central mass in the middle. These two different images may represent different orientations of F_0 in the membranes. In the reconstituted F_0F_1 complex, the F_0 sector could not be detected, because it was not possible to image, at the same time, two different objects with very different heights of ~100 Å (F_0F_1) and ≤10 Å (F_0) due to technical limitations. (C,D) Three-dimensional representation of F_0F_1 (C) and F_0 (D) in an area (125×125 nm) of reconstituted membranes selected from A and B, respectively. Surface plot program of Nanoscope III was used.

close look at the individual molecules revealed that half of the F_0 population had a central mass. The height of the central mass from the surface of the membrane was essentially the same as that of the surrounding structures.

.2. Critical evaluation of the dimensions of AFM images

The actual height of an isolated complex can be determined from an AFM image, as indicated in Fig. 2A: regardless of the finite dimensions of the scanning tip, the measured height (~100 Å) of F_0F_1 complexes on AFM should reflect the real height of the sample assuming that flattening of the sample is minimal. The values are in good agreement with those estimated on electron microscopy [4–6]. However, the apparent horizontal dimensions of well isolated molecules determined by AFM are generally much larger than the actual dimensions for the following reasons: (i) The force exerted by the AFM tip is large enough to flatten the sample [15]. (ii) The measured horizontal dimensions of samples depend on the radius of the curvature of the scanning tip and the actual height of the sample, as shown schematically in Fig. 2A. In particular, the outer diameters of samples are exaggerated, with an unavoidable large edge effect (Fig. 2A). The relationship between

Table 1
Two types of F_0 images obtained on AFM

	F_0 with a central hollow	F_0 with a central mass
Outer diameter	175±16 (~130)	177±12 (~130)
Inner diameter	43±8	40±3
Depth of hollow	18±2[a]	
Height of central mass		5±1
Major ridge width	87±7	81±4
Major ridge height	6±2	7±3
Minor ridge width	48±1	51±4
Minor ridge height	5±1	6±1

Mean values (Å) with standard deviations are shown for the dimensions of the two F_0 images. These values were obtained from AFM images for three separate F_0 specimens (15 images for each specimen). Corrected values are shown in parentheses for the outer diameters.
[a]Minimum possible dimension for depth due to the limitations of the AFM technique (see Fig. 2B).

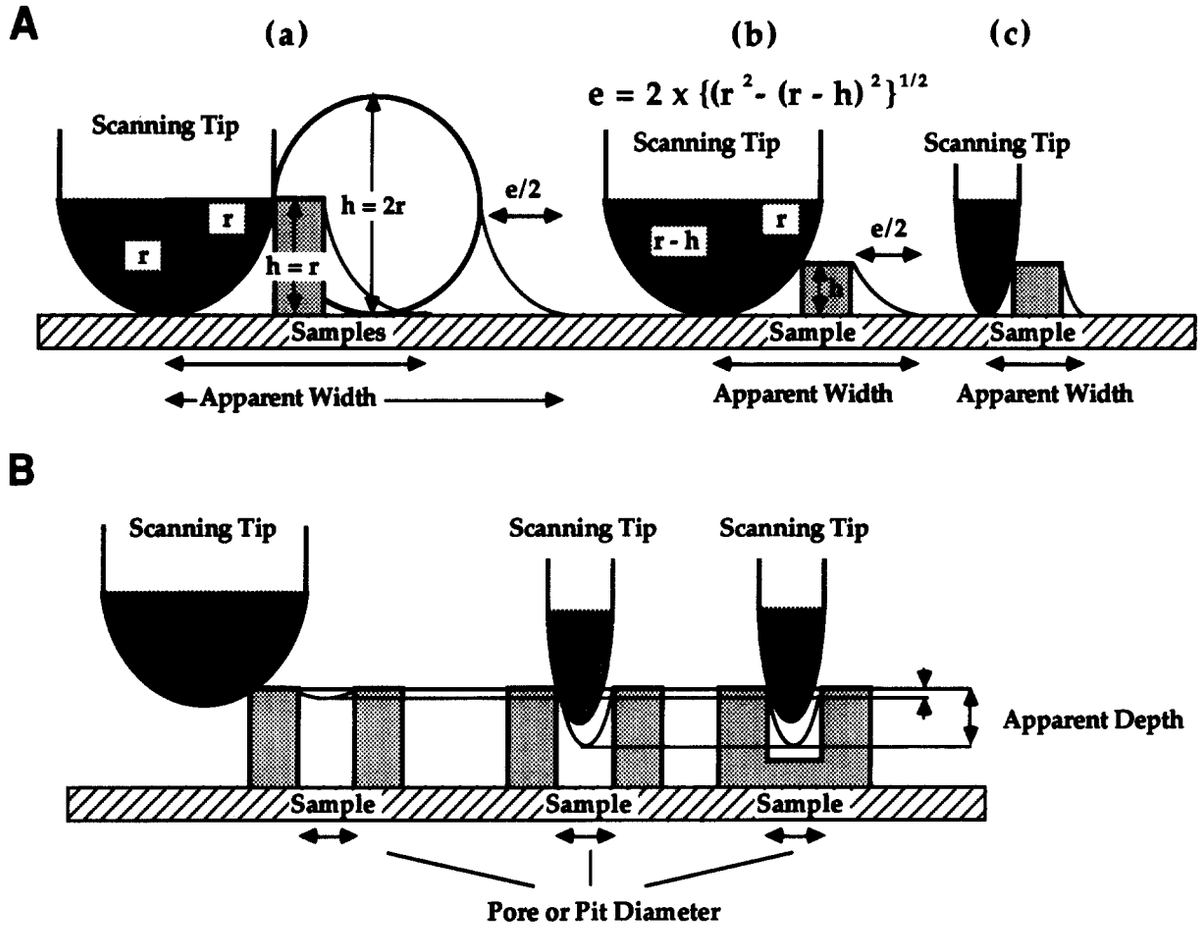

Fig. 2. Relationship between the curvature of the scanning tip and the apparent dimensions obtained by scanning a specimen. Tip movement in vertical direction during a scan in horizontal direction is used as information about the height and width of the specimen. (A) Schematic representation of two tips with different curvatures imaging different samples. The measured horizontal dimension (apparent width) involves an 'edge-effect' that prevents the scanning tip from gaining access to the edge of the sample. The measured horizontal dimension depends on the radius of curvature of the tip (b,c) and the height of the sample (a,b). The relationship between the error in the width (e), the radius of curvature (r) of the scanning tip and the height of the sample (h) is shown. The measured height, which is not dependent on tip dimensions in the case of well isolated samples, represents the real dimension. In the case of globular samples of height twice that of the radius of curvature of the tip (as in the case of the F_1 sector), the error will be the same as that of a rectangular sample of height equal to the radius of the globular sample (see a). (B) Schematic representation of the case in which a pore (or pit) is scanned with two different tips, showing that the both tips will give the same inner diameter, but different apparent depth. AFM cannot distinguish between a pit and a pore (compare second and third examples).

the error in horizontal dimensions (e), the radius of curvature of the tip (r) and the height of the sample (h) is given by

$$e = 2\times\{(r^2-(r-h)^2\}^{1/2} \quad (1)$$

However, when $h \geq r$, the equation is not valid, and a constant error ($2\times r$) would be obtained (Fig. 2A, right). The diameter of one F_1 sphere determined directly from the image was 187 ± 24 Å (mean ± S.D. for three preparations, 25 images for each preparation being inspected). The curvature of the AFM tip used for this scan was estimated to be ~50 Å by imaging DNA double helix of 20 Å diameter [16]. Since the height of the F_1 sector (97 Å) was greater than the radius of curvature of the tip, a possible real diameter of the F_1 sector (~90 Å) was obtained. This calculated dimension and the measured height (~100 Å), as well as the overall shape of a single molecule (one sphere), are consistent with the structural information obtained on electron microscopy of F_0F_1-ATPase and through X-ray diffraction studies on the F_1 catalytic subunit assembly [7,8], and support the idea that the images obtained represent the top views of F_1 sectors.

Two distinct ring-like images of F_0 sectors with outer diameters of 170–180 Å were obtained (Fig. 1B,D). Considering the height of the ring (6 Å) (Table 1) and the apparent changes in dimensions due to the curvature of the scanning tip used (Fig. 2A), the real outer diameter of the F_0 sector ring could be estimated to be ~130 Å (Eq. 1). It is important to note that, in contrast to the outer diameter of the F_0 sector, the diameter of the pore (~40 Å) determined by AFM should correspond roughly to the real dimension, since the error due to tip dimension is very small and negligible when compared to the error in outer dimension as shown schematically in Fig. 2B. In addition, the depth obtained from AFM images is the least possible depth (Fig. 2B), and the real depth is always

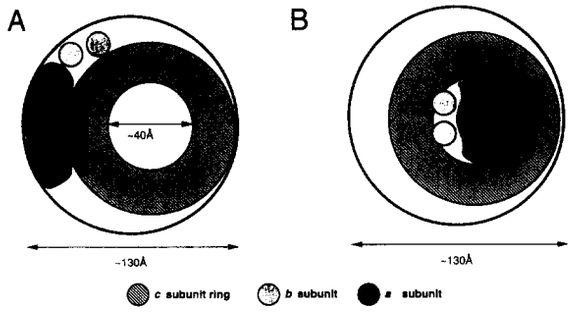

Fig. 3. Schematic models of the subunit assembly of F_0. The thick solid lines represent the boundaries of the F_0 sectors that are identified by AFM. Model A may be consistent with an assembly having outer and inner diameters of 130 and 40 Å, respectively. The *a* and *b* subunits directly contribute to the asymmetry of the ring-like structure consisting of the *c* subunits. Model B suffers from a disagreement of the space occupied by the *c* subunits with the area of the ring-like structure of F_0 obtained from AFM images. It is hard to explain using this model how a central hollow can be formed.

equal to or greater than the measured dimension. Thus, a pit and a pore cannot be distinguished by AFM imaging unless the other side is imaged as in this study.

3.3. Molecular organization of the F_0 sector

According to the AFM images, F_0 seems to be an inherently asymmetric assembly in the following two aspects. First, two kinds of ring-like structures were consistently observed; one with a hollow (depth ≥ 18 Å) in the middle, and the other with a central mass (Fig. 1B,D). These images possibly represent two surface views of F_0 oriented differently in the reconstituted membrane. Second, further analysis of these two ring-like structures at higher resolution (Fig. 1D) revealed that, in both types of rings, one half of the ring was about twice as thick as the other half (Table 1), although both halves (ridges) of the ring-like structures exhibited similar heights (< 10 Å). Such asymmetry of the F_0 sector was also found in a recent electron microscopic study [17]. It is noteworthy that, regardless of the presence of a central mass, a similar ring structure was observed in this study (Table 1).

The two asymmetric AFM images suggest a possible structure of F_0 comprising *a*, *b* and *c* subunits having 6, 1 and 2 transmembrane helices, respectively [1,2,10]. The central mass of the ring-like image may not represent the transmembrane helices of these subunits because other images showed a hollow (depth ≥ 18 Å). Thus, a model with central *a* and *b* subunits surrounded by 10–12 copies of the *c* subunit is unlikely (Fig. 3B).

In our model, the *a* and *b* subunits are attached to the ring-like structure formed by the *c* subunits (Fig. 3A). This allows at least 12 *c* subunits to form a symmetrical ring, taking into account the fact that each *c* subunit contains two transmembrane α helices (total 24 α helices for 12 *c* subunits). An asymmetric F_0 structure could be formed through the association with *a* and *b* subunits to one side of the symmetric ring formed by the *c* subunits. About 15 residues at the cytoplasmic amino terminus of the *c* subunit may extend beyond one side of the membrane, and form the central mass observed in a ring-like structure. Subunit *b* crosses the membrane with a single transmembrane helix, leaving most of the protein exposed to the cytoplasm [2,10]. However, such a structure could not be observed on AFM, although the F_0 preparation contained a stoichiometric amount of subunit *b*. Thus, it may be possible that the *b* subunit could not be maintained as part of the stalk and thus formed the central mass observed on AFM.

Acknowledgements: This work was supported by grants from NIH (GM44373) to K.T., and from the Japanese Ministry of Education, Science and Culture, and the Human Frontier Science Program to M.F. K.T. is an Established Investigator of the American Heart Association. We are grateful to Mr. J.K. Paul for technical assistance.

References

[1] Futai, M., Noumi, T. and Maeda, M. (1989) Annu. Rev. Biochem. 58, 111–136.
[2] Fillingame, R.H. (1990) The Bacteria, vol. 7 (Krulwich, T.A. ed.) pp. 345–391, Academic Press, New York.
[3] Penefsky, H.S. and Cross, R.L. (1991) Adv. Enzymol. 64, 173–213.
[4] Gogol, E.P., Johnston, E., Aggeler, F. and Capaldi, R.A. (1990) Proc. Natl. Acad. Sci. USA 87, 9585–9589.
[5] Gogol, E.P., Aggeler, R., Sagermann, M. and Capaldi, R.A. (1989) Biochemistry 28, 4717–4724.
[6] Lücken, U., Gogol, E.P. and Capaldi, R.A. (1990) Biochemistry 29, 5339–5343.
[7] Abrahams, J.P., Leslie, A.G.W., Lutter, R. and Walker, J.E. (1994) Nature 370, 621–628.
[8] Bianchet, M., Ysern, X., Hullihen, J., Pedersen, P.L. and Amzel, L.M. (1991) J. Biol. Chem. 266, 22197–22201.
[9] Boyer, P.D. (1993) Biochim. Biophys. Acta 1140, 215–250.
[10] Schneider, E. and Altendolf, K. (1987) Microbiol. Rev. 51, 477–497.
[11] Girvin, M.E. and Fillingame, R.H. (1994) Biochemistry 33, 665–674.
[12] Girvin, M.E. and Fillingame, R.H. (1995) Biochemistry 34, 1635–1645.
[13] Moriyama, Y., Iwamoto, A., Hanada, H., Maeda, M. and Futai, M. (1991) J. Biol. Chem. 266, 22141–22146.
[14] Sone, N., Yoshida, M., Hirata, H. and Kagawa, Y. (1978) Proc. Natl. Sci. USA 75, 4219–4223.
[15] Paul, J.K., Nettikadan, S.R., Ganjeizadeh, M., Yamaguchi, M. and Takeyasu, K. (1994) FEBS Lett. 346, 289–294.
[16] Bustamonte, C., Keller, D. and Yang, G. (1993) Curr. Opinion Struct. Biol. 3, 363–372.
[17] Birkenhäger, R., Hoppert, M., Deckers-Hebestreit, G., Mayer, F. and Altendorf, K. (1995) Eur. J. Biochem. 230, 58–67.